New UV-LED frontal flow photocatalytic reactor for VOCs treatment: Compactness, intensification and optimization studies

Youcef Serhane, Abdelkrim Bouzaza, Dominique Wolbert, Aymen Amin Assadi

Conception of new compact frontal flow photocatalytic reactor based on luminous textiles with high energy efficiency: Intensification and optimization studies toward gas pollutant elimination

Youcef Serhane[a], Abdelkrim Bouzaza[a], Dominique Wolbert[a], Aymen Amin Assadi[a,*]

[a] Univ Rennes, École Nationale Supérieure de Chimie de Rennes, CNRS, ISCR (Institut des Sciences Chimiques de Rennes) – UMR 6226, F-35000 Rennes, France

*Corresponding author. Tel: +33(0)223238152, Fax: +33(0)223238120,

E-mail: Aymen.assadi@ensc-rennes.fr

Abstract

A solution for the optimization of the photocatalytic treatment of toxic gases based on the use of TiO_2 media deposited on luminous textile, was studied and implemented. Cyclohexane was chosen as a reference for the type A gas filter tests. The photocatalytic media were firstly characterized by scanning electron microscopy (SEM). Then, the experiments carried out on a batch reactor showed that the TiO_2 coated optical fiber media gives better performances than conventional TiO_2 deposited on cellulosic fiber support. In order to take advantage of the new configuration based on optical fiber media, an intensification study was carried out by increasing the amount of TiO_2 in the media, and UV intensities of LED. The increase of these two parameters leads to a process degradation rate of about 4 times higher. The continuous treatment allowed the efficiency of the new configuration of the front flow reactors developed (PFR-LED) to be highlighted, in comparison with the

conventional configuration. This is interpreted in the increase of the specific degradation rate of the optimized PFR-LED by four times compared to the conventional reactor. The performance evaluation of the compact and optimized configuration of the frontal flow reactor (PFR-LED Optimized), aimed at highlighting the influence of the inlet concentration under different flow rates. In addition, the effect of the number of optical fibers support shows that the degradation rate and selectivity are enhanced. The main rates obtained were for a cyclohexane input concentration of 1.19 mmol.m^{-3} in optimal humid condition (38%) at an air flow rate of 18 L min^{-1} with four photocatalytic media (4OF/4UV-LED), where the CO_2 selectivity reached 31% for an abatement of 59%.

This global investigation, has mainly allowed the design of a new version of compact reactor. A version as economical as efficient in terms of elimination of gaseous pollutants which clearly meets the main goals of sustainable development.

Keywords

Air treatment; Front flow photocatalytic reactor; kinetic modelling; Compactness; Intensification; Optimization.

1. Introduction

Indoor and outdoor air pollution has become a real concern in today's world. Outside pollution is caused by many factors, sometimes natural such as volcanic air pollution [1]. But most often air pollution is of human origin, namely the pollution released by the large number of vehicles as well as by industries [2]. Inside, the air is also polluted in a specific way by potential sources (combustion devices, construction materials, decoration products) and also human activity (smoking, cleaning products, cooking,..) [3,4]. When this air, constituting a wide variety of volatile organic

compounds (VOCs), is breathed in by humans, it results in respiratory problems and lung cancer [1][2].

On this context, photocatalysis can be considered as a promising solution for air purification [3–7]. This process allows the mineralization of many organic compounds at room temperature using a semiconductor, namely TiO_2 (high photoactivity, chemical stability and low cost) and an ultraviolet source to decompose VOCs through consecutive oxidation reactions and produce CO_2, H_2O and other by-products [4-8].

Continuous reactors, equipped by immobilized catalyst, are most frequently used in air purification [10,11][12][13]. However, as reported in the literature [14], many disadvantages come into play when a fixed photocatalyst system is implemented. On the one hand, it is necessary to illuminate a large surface of the photocatalyst. The loss of photons due to the absorption of the UV radiation by the support leads to a decrease efficiency of the catalyst. On the other hand, another crucial disadvantage of this process, is the use of a UV lamp as a light source. Due to the lamp size, the reactor volume , as well as the high energy consumption [15,16] became an obstacle in the reactor design. New reactor designs based on optical fibers as a support for the photocatalyst have been developed and tested to overcome these problems. These reactors lead to an improvement of the photocatalytic efficiency due to better contact between the catalyst, the light and the pollutant [14–18][21] [22]. However, less mass transfer is observed under parallel configuration. [23]. Faced with this disadvantage, frontal flow photocatalytic reactors present an efficient solution, as this configuration allows to play on the compactness of the reactor for the treatment of air at high flow rates by favoring the mass transfer [24][25][26].

The aim of our contribution concerns the design of a new frontal flow reactor for the treatment of polluted air by optical fibers textile developed by the company Brochier Technologies-France. A particularly innovative aspect of this illuminated textile is the simultaneous weaving of textile and optical fibers, allowing the frontal flow photocatalytic reactor to have a very compact design. Therefore, the illuminated textile is considered both as a support for the TiO_2 and as a transmitter of light through the optical fibers from the source to the catalyst surface. Thus, it combines the maximization of the interactions between the pollutant and the catalyst surface with a very large illumination area of the catalyst surface (maximization of the interactions between the light and the catalyst surface) [23,27–29]. In addition, this configuration allows the reactor size to be reduced compared to conventional reactors (process intensification), with less energy consumed [23,30,31].

In this study, a comparison between new and conventional configurations was highlighted. Firstly, in a batch system where Langmuir-Hinshelwood model was applied to represent the kinetics and compare the potential of the light fabric to the conventional heterogeneous photocatalysis process, i.e. using TiO_2 deposited on cellulose paper based on activation by an external UV lamp. Followed by a degradation efficiency comparison of the front-flow photocatalytic reactors configurations, considering energy consumption with special attention to the reactor compactness. In addition, the parameters of the new frontal flow photocatalytic reactor based on optical fiber media were optimized, in order to further enhance its photocatalytic efficiency and to confirm its ability to treat pollutants under the influence of the operating conditions, i.e. inlet concentration, flow rate and relative humidity as well as the number of photocatalytic medias.

It should be noted that the established literature review does not show any work on this new configuration based on the sustainable development goals, even on its intensification.

2. Material and methods

2.1. Pollutant studied

In this study, cyclohexane was used as a target pollutant. It is supplied by Sigma-Aldrich/Germany, in liquid form (purity > 98%), volatilized afterwards to obtain the desired gas concentrations.

2.2. Photocatalytic support

Two photocatalytic supports were used in this study (Fig. 1). The first one is a media provided by the Ahlström Paper Group, where the conditioning was achieved by an aqueous suspension of a mixture of TiO_2 (Millennium PC 500) and silica, deposited on a non-woven fibrous support of synthetic and natural cellulose. A winding press process was used to coat the fibers by fixing TiO_2 to different substrates. The colloidal silica used has a specific surface area of about 700 $m^2.g^{-1}$, with elementary particles of 20-30 nm in diameter. It acts as an inorganic binder, resistant to UV radiation and photocatalysis, transparent to UV and protecting the fibers. The titanium dioxide then forms agglomerates of varying size (0.1 to 1 µm). More details on this photocatalytic media have been presented in our previous publications [31][32][33].

The second is a new double-sided photocatalytic media, manufactured by Brochier Technologies (UVtex®). Based on the combination of plastic optical fibers (OF) (polymethylmethacrylate) around which textile fibers (polyester, Trevira CS TM fibers) are wound. The OFs have an average diameter of about 500 µm. Indeed, the core of

the OF is formed by a polymethyl methacrylate resin with an average diameter of 480 µm and covered with a 10 µm thick fluoropolymer [29]. These optical fibers are treated to transmit and emit light laterally on their outer surface. For a textile sample, all OFs are collected at one end in an aluminum connector. The luminous textile is covered with a layer of silica that serves as a protection against degradation during the photocatalytic process. However, silica was chosen because it allows UV light transmittance, and being a non-organic compound, it is not degraded by photocatalysis [28]. The textile fiber is soaked for 60 min in a stirred suspension containing TiO_2 Degussa P25 powder (50 $g.L^{-1}$), then dried for 2 h at 70 C°. At the end of this process, 12 $g.m^{-2}$ of TiO_2 are uniformly distributed on the textile fiber. More information are mentioned in our previous publications [23,27].

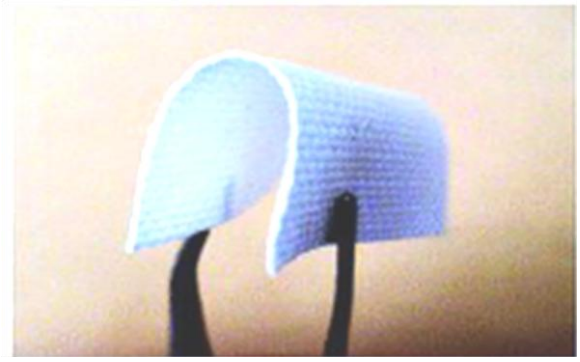

TiO_2 deposited on Cellulosic support

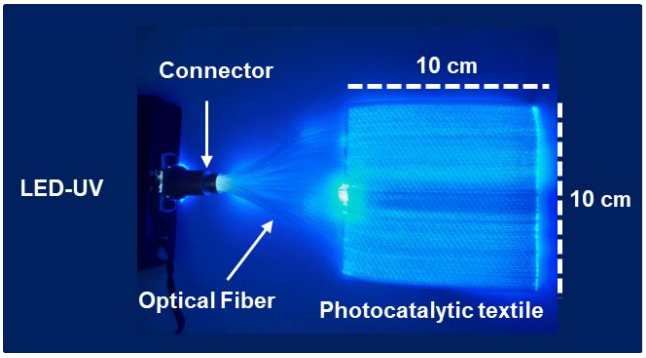

TiO_2 coated on Optical Fibers

(a) **(b)** **(c)**

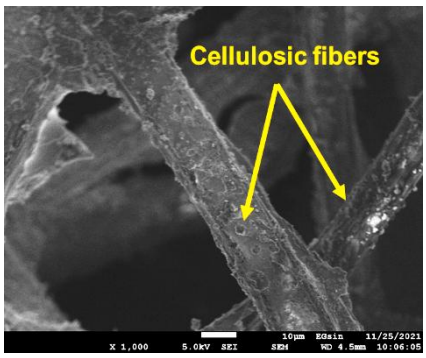

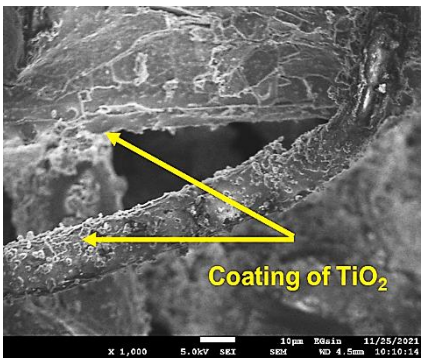

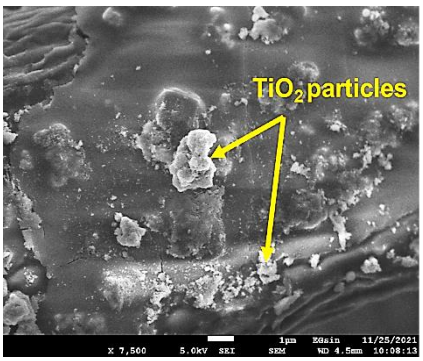

(d) (e) (f)

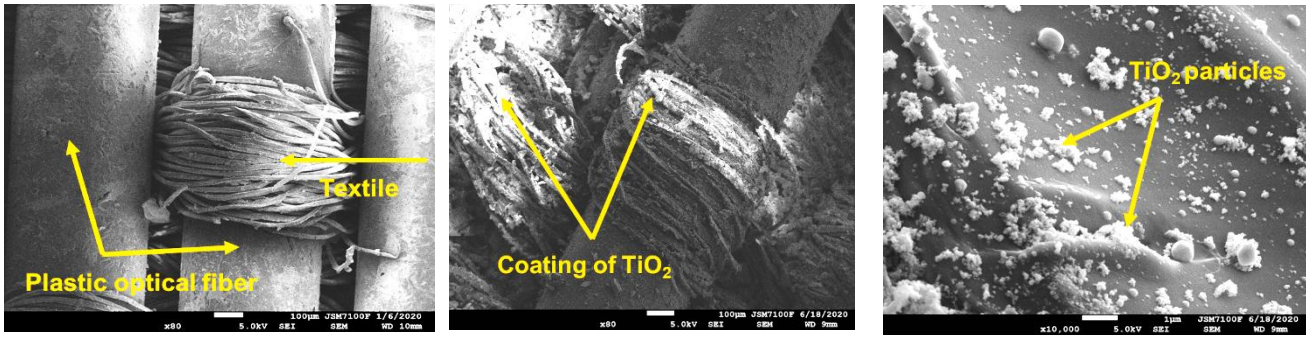

Figure 1: SEM pictures of photocatalytic materials: (a, b and c) TiO_2 deposited on cellulosic support, (d, e and f) TiO_2 coated Optical fiber media.

Details of the surface texture characterization of the cellulosic and OF supports were analyzed by scanning electron microscopy (SEM- JEOL JSM 7100F). Figure 1 (a, b and c) shows the location of the TiO_2 particles deposited on the cellulosic fibers. As described in our previous work [23,27], figure 1 (d, e and f) shows OFs on which TiO_2 nanoparticles have been coated. The OF is knitted, according to the Jacquard process, i.e. the interweaving of fibers are placed in the direction of the textile fibers (chain), and of some fibers which are placed perpendicular to the fibers of the warp, in the direction of the OF (Fig. 1 d, and e). As shown in Fig. 1.e, a coating layer of TiO_2 is present on the textile fiber and the starting threads. Therefore, this allows a large amount of TiO_2 to be activated, which will improve the photocatalytic efficiency.

2.3. Reactor and experimental set-up:

2.3.1. Batch reactors

In this study, two types of photoreactor were used. The first one is a conventional reactor (Fig. 2a) which contains a central tube for the installation of the fluorescent

UV lamp (Philips PL-L 24W/10/4P) which allows the activation of the cellulose photocatalytic support deposited on the inner wall of the reactor. It is approximately 40 cm high and has a volume of 1.5 L. The UV intensity of the lamp is measured by a VLX-3W radiometer equipped with a CX-365 cell. The second is a reactor with a luminous textile (Fig.2b) with a surface of 10*10 cm containing a quantity of TiO_2 equal to 10 $g.m^{-2}$. UVA-LED type (Bin N) connected to a dimmer supplied by Brochier technologies (Lightex) was used to ensure a good distribution of the radiation on the surface catalyst through the fiber filaments.

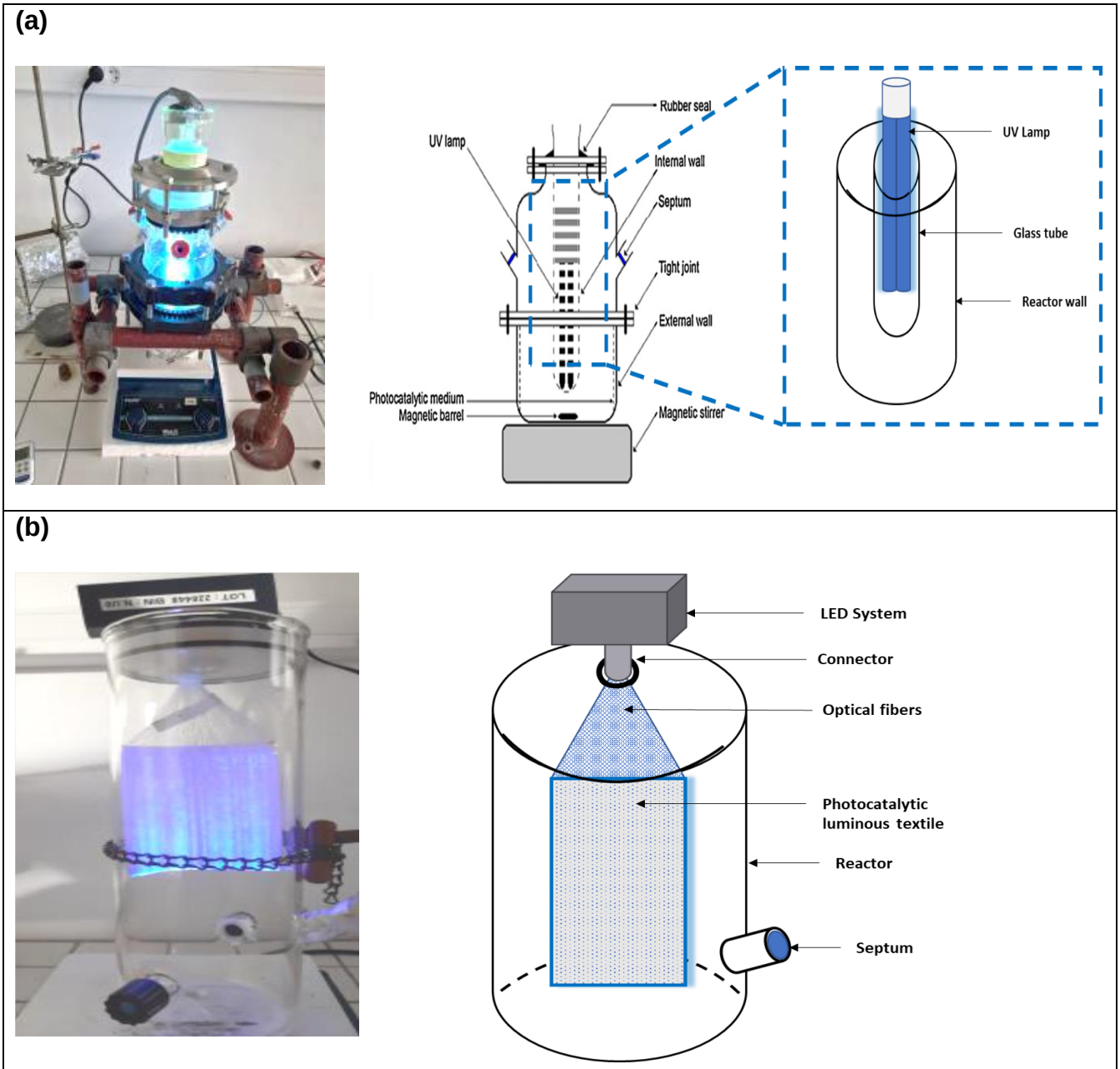

Figure 2: Photo and schema of batch reactors: (a) conventional configuration based on cellulosic media, (b) Optical fiber (luminous textile) configuration.

156

157 The major differences between the two reactors were the light intensity and reactor
158 volume used, which were greater with the conventional photocatalytic plant. This was
159 due to the use of external light source positioned vertically in the reactor to activate
160 the TiO_2 deposited on the cellulose paper.

To generate pollution in the reactor, the pollutant is injected in the form of liquid drops which then evaporate. A magnetic stirrer is used to homogenize the gases.

2.3.2. Continuous process

The classic front flow photocatalytic reactor, namely (P50) is illustrated in Fig. 3a, with a passage section of 0.01 m^2 and a total volume of about 4 L. It is formed by four mountable stainless-steel test chambers, containing four Cellulosic photocatalytic media (4 x 0.01 m^2 of surface giving 0.64 g of TiO_2) and two Philips UV-A lamps (model PLS 9W / 10). The intensity of the light incident at 365 nm on the surface of the catalyst is 20 W/m^2 which is measured by the radiometer “VLX 3 W”).

The second reactor represents a new configuration (Fig. 3b), recently developed and built to work in frontal flow. The reactor is composed of modules adapted for the installation of TiO_2 on OF media, ensuring a passage section similar to that of the classic reactor (about 10 cm^2). Made of Bakelite, which gives it a high mechanical resistance (hard, rigid), and good electrical insulation and temperature resistance (120 C° continuously). Bakelite is also not influenced by photocatalysis and UV light. The objective of this configuration is to optimize the photocatalytic treatment by reducing the residence time, while ensuring good degradation efficiency. This last configuration has been developed in two ways. The first one was based on OF media loaded with 10 $g.m^{-2}$ of TiO_2, with an UV Intensity of 1.5 $W.m^{-2}$, namely Photocatalytic Filtring Reactor-LED (PFR-LED). The second one, in order to optimize the photocatalytic treatment process, consists of an OF media containing 26 $g.m^{-2}$ of TiO_2, with an applied UV Intensity about 2.6 W.m-2 called PFR-LED Optimized.

183 It should be noted, that the electrical energy consumed and required for the
184 photocatalytic process for each reactor, was measured using an energy cost meter
185 (ENERGY LOGGER 4000F) of the manufacturer VOLTCRAFT®.

(a)

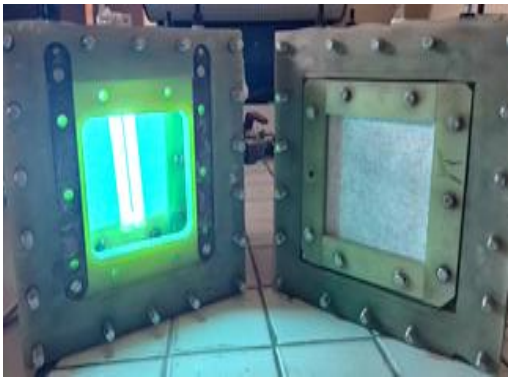

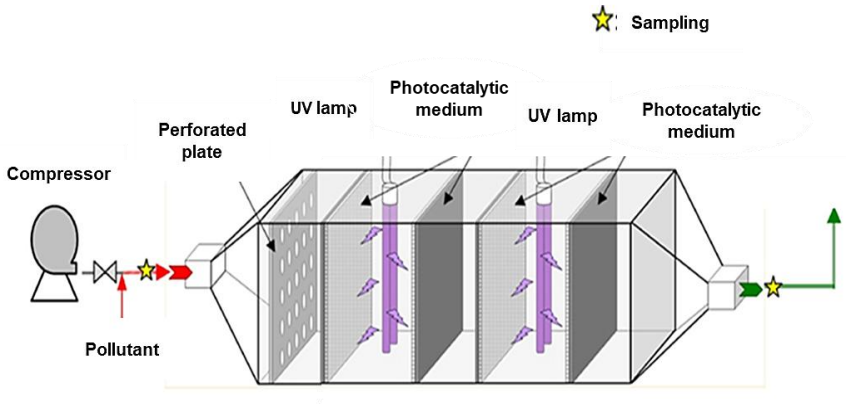

Classic configuration - Outdoor lighting (UV lamp)

(b)

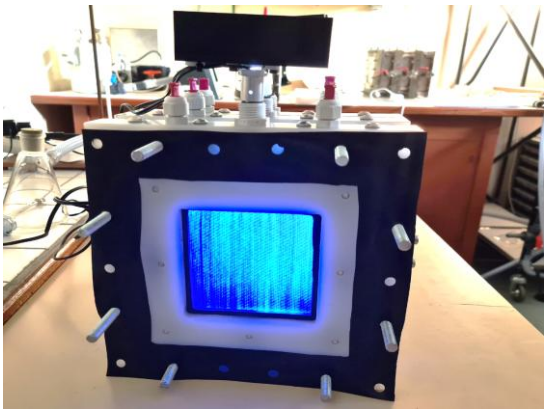

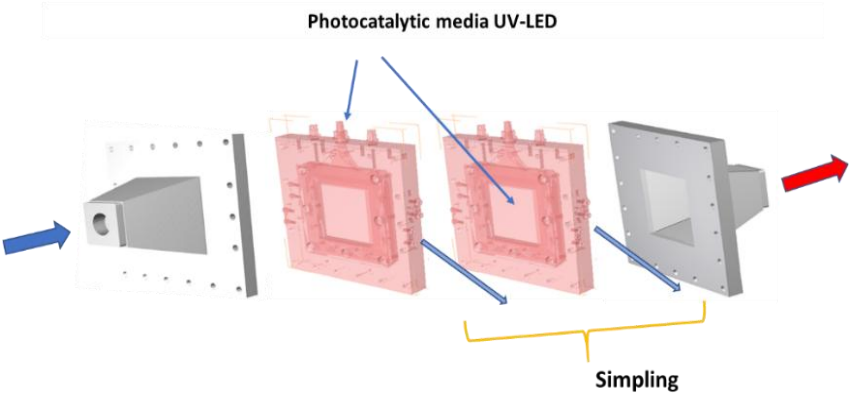

New configuration - *In-situ* lighting (UV-LED)

Figure 3: (a) Front flow photocatalytic reactor based on cellulosic media (P50); (b) Front-flow reactor based optical fibers photocatalytic media (PFR-LED)

186

187

188

The main characteristics of the different reactors and configurations are presented in Table 1.

Characteristics	rectors		
	P50	**PFR-LED**	**PFR-LED Optimized**
Volume (m^3)	4.10^{-3}	$1,2.10^{-3}$	$1,2.10^{-3}$
Compactness ($m^2.m^{-3}$)	2.5	11.11	11.11
Masse TiO_2 ($g.m^{-2}$)	64	3	78
UV intensity ($W.m^{-2}$)	20	4.5	7.8
Energy consumed (watt)	31.1	14.5	15.7

Table 1: Characteristics comparison of frontal flow photocatalytic reactors

2.3.2.1. Experimental setup:

The appropriate reactor for the test is installed in each case. Dry air from the network is sent as the carrier gas, controlled by a valve and a Gallus G4 gas meter of the Itrón brand. The flow rates tested are equal to 13, 18 and 36 $L.min^{-1}$. These flow rates correspond to contact times of 18, 13 and 7 ms respectively. To humidify the air, a bubbler was installed in the circuit containing water to achieve humidity ranges of 5-80%. The pollutant is injected continuously in liquid form by a syringe / syringe pump combination. A heating tape, is placed in the injection zone to facilitate the volatilization of the pollutant and a static mixer makes it possible to homogenize the effluent upstream of the photoreactor. Two septa downstream and upstream of the photoreactor make it possible to sample the outlet and inlet gas with a syringe (Fig.4).

Once the adsorption process reaches equilibrium (depending on the concentration), as indicated by an identical input / output Volatile Organic Compound concentration, the UV lighting is turned on. A transient period precedes a steady state phase which is established when the concentration of pollutant at the outlet becomes constant.

The reactor is rinsed under UV light for 1 h in ambient air after each experimental sequence. or it is useful to report that no deactivation has been observed.

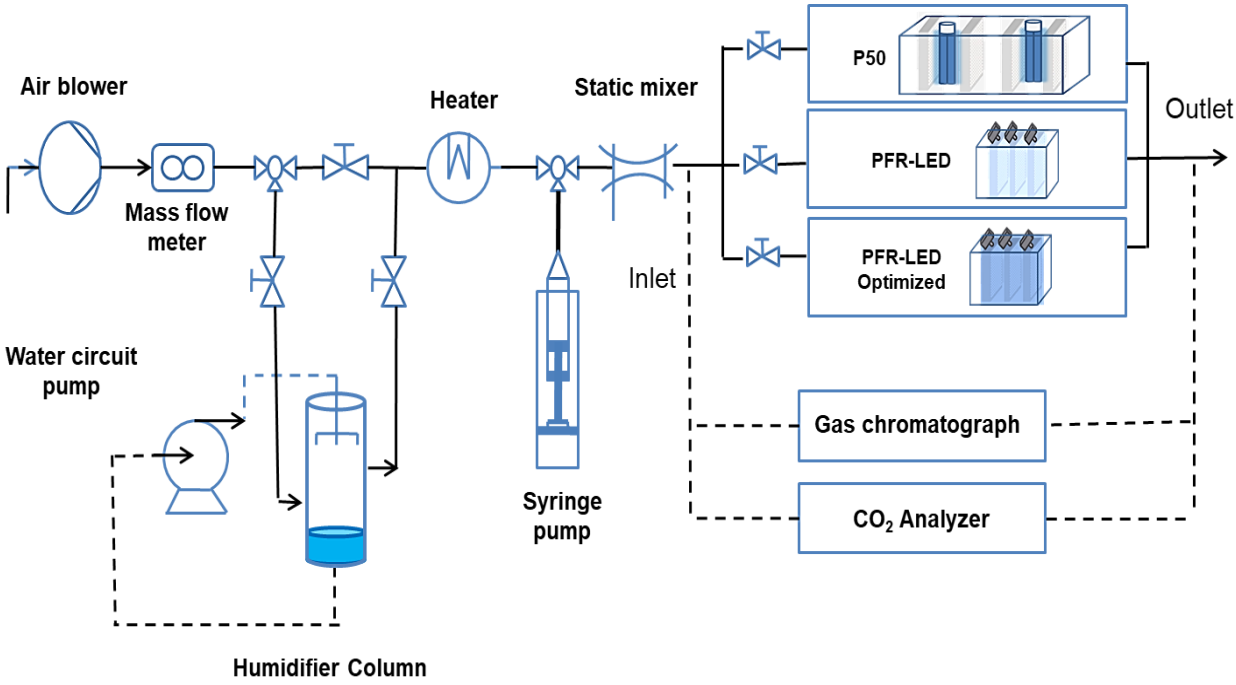

Figure 4: Diagram of the continuous photocatalytic process treatment for the three reactors

2.3.2.2. Analytic tools

The concentration of cyclohexane was measured by a Thermo electron corporation gas chromatography (Focus GC) using a flame ionization detector (FID) and an FFAP column (length = 25 m and internal diameter = 0, 32 mm). Nitrogen was used as a carrier gas. The temperature conditions of the oven, the injection chamber and the detector were, respectively, 50, 190 and 190 °C. The analysis was performed by

direct manual sampling with a 500 µl syringe and injection into the GC. The calibration was carried out by evaporating different quantities of cyclohexane on a closed bottle. The correlation of the pollutant with a peak area of GC-FID as a function of its concentration was carried out. Operation is done by Azur™ software.

The CO_2 was analyzed by a Fourier transform infrared spectrophotometer (FTIR) from Environment SA (MIR 9000H).

3. Results and discussions

3.1. Photocatalytic performance of catalysts

The objective of this study is to highlight the performance of the two studied photocatalytic media, cellulosic and OF. For a better evaluation, the efficiency of the media was regarded in terms of the photocatalytic degradation rate represented by the Langmuir-Hinshelwood model (Eq.1), which considers the contribution of the adsorption properties of the pollutant on the catalyst surface and the kinetics of the photocatalytic reactions [34][35][36]. Due to the complex mechanism of the reactions, the L-H model is only applied at the beginning of the treatment in order to avoid the influence of intermediate by-products on the photocatalytic removal of cyclohexane. As already reported in the literature, the reaction rate constant (k) and adsorption constant (K) can be determined using Eq.2.

$$r_0 = \frac{kKC_0}{1+KC_0} \qquad \text{(Eq. 1)}$$

$$Or \quad \frac{1}{r_0} = \frac{1}{kK}\frac{1}{C_0} + \frac{1}{k} \qquad \text{(Eq. 2)}$$

where r_0 is the initial reaction rate (mmol.m^{-3}.s^{-1}), k the reaction rate constant (mmol.m^{-3}.s^{-1}) and K is the adsorption constant (m^3.mmol^{-1}).

3.1.1. Comparison of the photocatalytic media

The performance of the cellulosic and OF media was investigated in terms of initial degradation rates (mmol.m^{-3}.s^{-1}), at different pollutant concentrations (mmol.m^{-3}), with the same amount of TiO_2 deposited in each media under the same UV intensity (Fig.5).

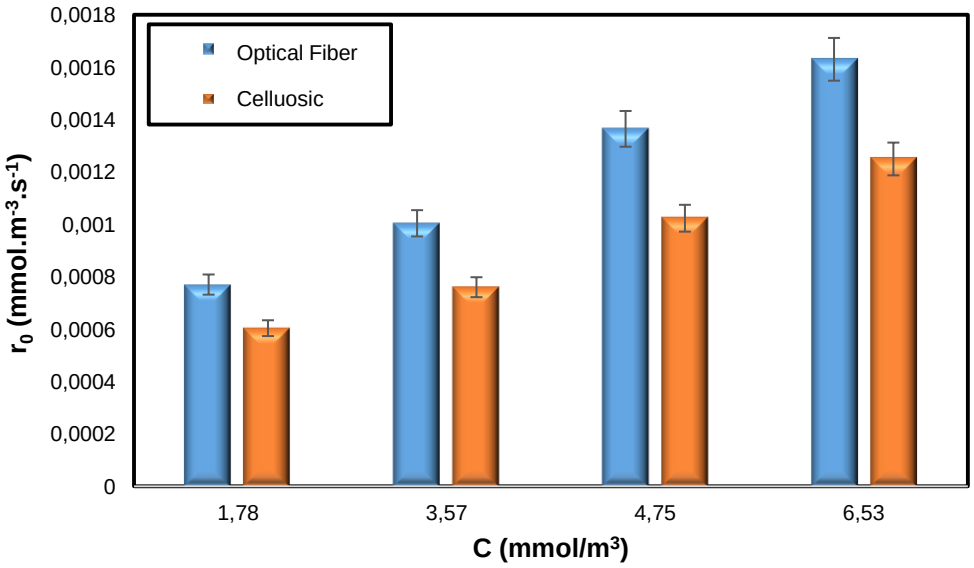

Figure 5: Initial degradation rate of Cyclohexane with Cellulosic and Optical fiber media at different concentrations (HR = 40 ± 2%, T = 20 ± 2 C°, UV Intensity = 1.5 W.m^{-2}, m_{TiO2} = 10 g.m^{-2})

Before even deciding on the performance of the two media, it is useful to note that the results (Fig. 5) show the same trends, where at low input concentration, the degradation follows pseudo first order kinetics where the degradation is proportional to the input concentration. This can be explained by the fact that not all active sites are occupied and that an increase in concentration generates a greater surface coverage which implies a better degradation rate [37].

We note that OF media gives a better degradation rate than Cellulosic one regardless of the initial concentration. Moreover, the improved efficiency of OF seems to be of the same order for all the initial concentrations tested.

Langmuir-Hinshelwood constants for the two medias were determined (table 2), to permit the comparison of the two media. Here, we note that experimental data fit well the model which means that the chemical reaction is the limiting step in the process [38][39].

Media	Cellulosic	Optical fiber
k_{app} (mmol.m^{-3}.s^{-1})	0.0027	0.0032
K (m^{3}.mmol^{-1})	0.128	0.144
R^2 (%)	99.75	99.63

Table 2: Value of Langmuir-Hinshelwood reaction rate constants (k) and Langmuir adsorption constants (K)

The results confirm that the way to apply the light intensity is the key parameter, which influences the performance of the photocatalytic processes. The OF media better treatment performance in terms of mmol removed is also reflected by an increase in the apparent kinetic constant (k) from 0.0027 to 0.0032 mmol.m^{-3}.s^{-1} for the cellulosic and OF media respectively, due to the *in-situ* illumination. In other words, for the same UV intensity, more active sites are created with the OF leading to more electrons and holes which explains the illumination performance translated by the percentage increase of the initial degradation rate compared to the conventional media which is about 23% [40].

3.1.2. Photocatalytic capacity intensification of the optical fiber media

3.1.2.a. Effect of mass of TiO_2

In order to increase the photocatalytic efficiency of the OF media, the mass of TiO_2 deposited on the photocatalytic media was investigated. To this purpose, the degradation rate was studied for three OF media with respective TiO_2 masses of the order of 10, 18 and 26 $g.m^{-2}$ by applying the same UV intensity (1.5 $W.m^{-2}$) at different concentrations.

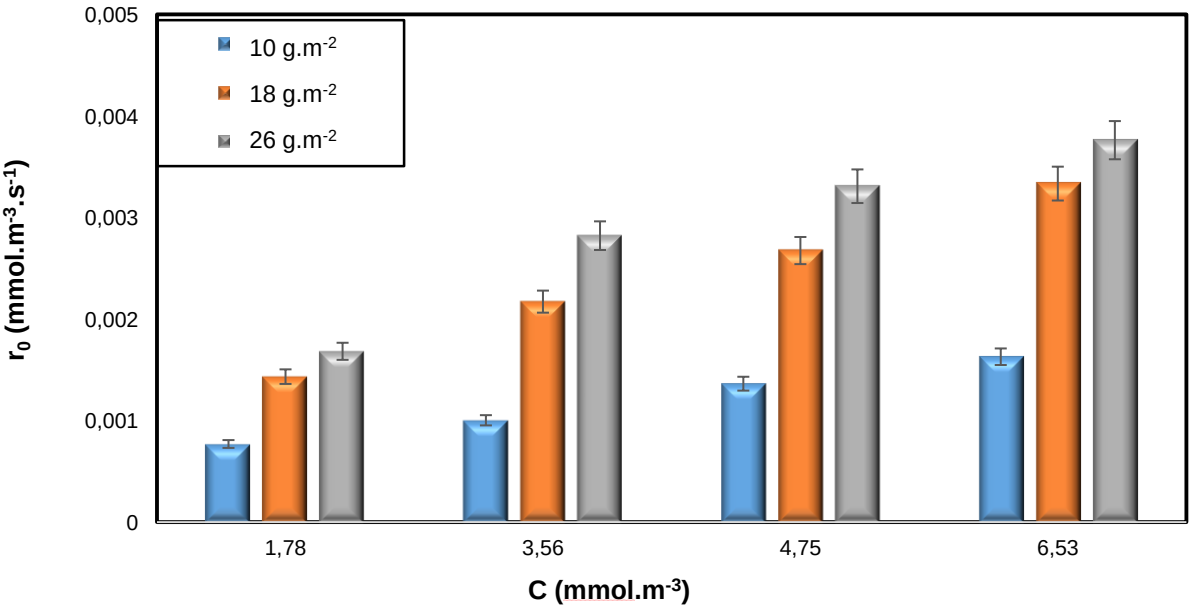

Figure 6: Initial degradation rate with different mass of TiO_2 on OF at different Cyclohexane concentrations. (HR = 40 ± 2%, T = 20 ± 2 C°, UV Intensity = 1.5 $W.m^{-2}$)

The results illustrated in Figure 6 show the variation of the initial rate for the removal of cyclohexane, with different OF media containing different amounts of TiO_2, under the same UV irradiation. It is observed that the rate of the reaction increases with the increase in the mass of TiO_2 deposited on the photocatalytic media, which can be explained by the fact, that the amount of catalyst increases the number of active sites on the photocatalyst surface, which in turn increases the number of hydroxyl and superoxide radicals [41–43]. Furthermore, it is found that the increase in reaction rate is not proportional to the increase in the amount of TiO_2 deposited in the medium. This is shown in Table 3, where the apparent kinetic constants obtained go from

285 0.0032 mmol.m^{-3}.s^{-1}, 0.0072 mmol.m^{-3}.s^{-1} for 10 and 18 g.m^{-2} which corresponds to
286 125% of increase on the other hand by passing from 18 to 26 g.m^{-2} it is recorded an
287 increase in the initial degradation rate of 15% (0.0072 to 0.0083 mmol.m^{-3}.s^{-1}). It is
288 also noted that the adsorption constant (K) is approximately constant. This can be
289 interpreted by the fact that not all photocatalytic sites are activated at high amount of
290 TiO_2 [44,45]. In other words, the increase of TiO_2 in the media must be accompanied
291 by an enough UV intensity for the activation of all photocatalytic sites. In our case the
292 increase of the catalyst load lead to an increase of the degradation rate. This means
293 that all the catalyst is activated and there is no limit due to mass transfer. However, it
294 is possible that the optimum amount of the catalyst will be reached where the
295 efficiency of the degradation rate per unit mass will decrease.

296 This is in agreement with the literature, especially the work of Alonso-Tellez et al. [46]
297 and Wang et al. [47], and also that of Vezzoli et al [48], where it is shown that a
298 further increase in mass of the catalyst leads to recombination of charge carriers at a
299 relatively small distance from the solid-gas interface, resulting in a decrease in the
300 reaction rate.

Mass of TiO_2 (g.m^{-2})	10	18	26
k_{app} (mmol.m^{-3}.s^{-1})	0,0032	0,0072	0,0083
K (m^3.$mmol^{-1}$)	0,1441	0,1074	0,1170
R^2 (%)	99,63	97,92	98,3

301 **Table 3**: Value of Langmuir-Hinshelwood reaction rate constants (k) and Langmuir
302 adsorption constants (K) for the degradation of Cyclohexane with different optical
303 fiber media with different mass of TiO_2 at different concentrations. (HR = 40 ± 2%, T
304 = 20 ± 2 C°, UV Intensity = 1.5 W.m^{-2})

305 **3.1.2.b. Effect of UV intensity**

In order to boost the photocatalytic efficiency of the OF media, the light intensity was studied as a crucial factor in influencing the reaction rate. For this purpose, the degradation rate was studied for an OF media containing 26 $mg.m^{-2}$ of TiO_2 (maximum mass) under different UV intensities (0.3 $W.m^{-2}$, 1.5 $W.m^{-2}$ and 2.6 $W.m^{-2}$) at different concentrations.

The results illustrated in figure 7 show a similar behavior to what has been reported in the literature regarding the effect of UV intensity, where the photocatalytic oxidation performance of the OF media improves as the light intensity increases [44,49]. This can be explained by the fact that increasing the intensity of UV light creates more photons, which enhance the production of oxidizing species [50–52].

In this study, the results of the apparent reaction kinetic constants (Tab. 4) show that the increase in intensity has overcome the limitation of the photocatalytic oxidation efficiency caused by the loading of the photocatalytic media with TiO_2. this is due to the efficiency of the illumination by *in-situ* UV LED lighting, overcoming the problems of shading and intensity loss [40].

According to the power relation law ($k_{app} = k_0.I^{\alpha}$). It is also noted that the photocatalytic reaction rate follows a first order regime with applied irradiation intensities, where α is about 0.64 with k_0 = 0.0064 $mmol.m^{-3}.s^{-1}$, meaning that the photogenerated electron-hole pairs are consumed more rapidly by chemical reaction than by recombination [44][53]. The results reported by some authors [50] [55][56][33] give a value varying from 0.25 to 0.5 when an external lighting is used. So, the use of OF seems to be me more efficient [51][57].

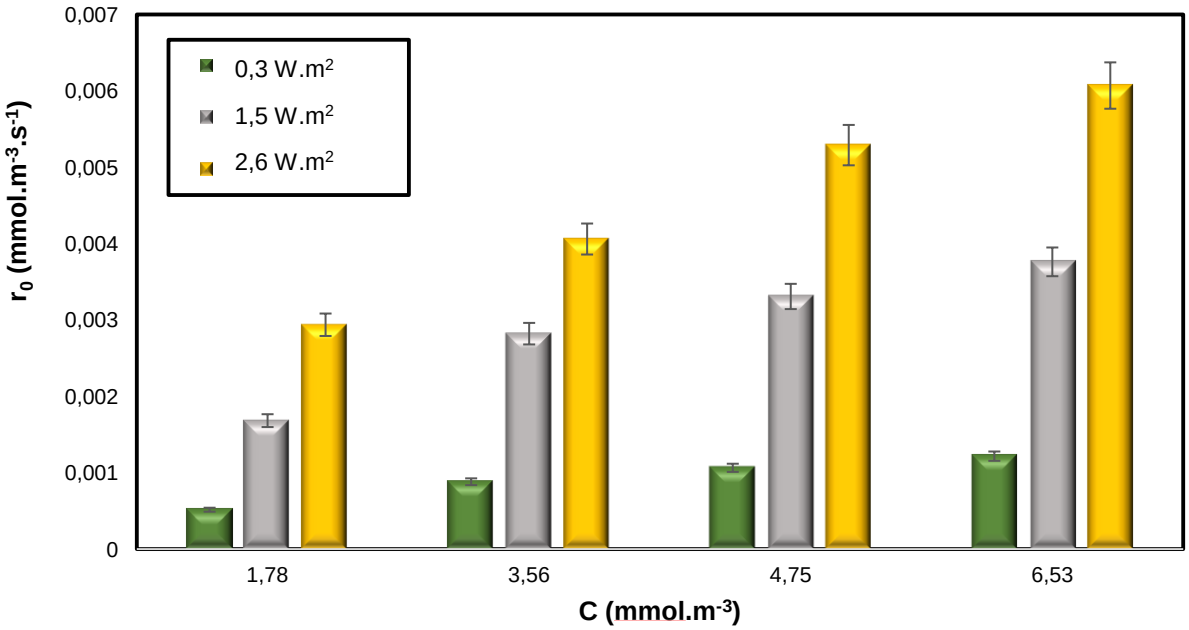

Figure 7: Initial degradation rate of Cyclohexane with optical fiber media at different concentrations under different UV Intensity (HR = 40 ± 2%, T = 20 ± 2 C°, m_{TiO2} = 26 g.m^{-2})

UV Intensity (W.m^{-2})	0,3	1,5	2,6
k_{app} (mmol.m^{-3}.s^{-1})	0,0032	0,0083	0,0118
K (m^3.mmol^{-1})	0,0903	0,1170	0,1284
R^2 (%)	98,36	98,3	97,48

Table 4: Value of Langmuir-Hinshelwood reaction rate constants (k) and Langmuir adsorption constants (K) for the degradation of Cyclohexane under different UV Intensity (HR = 40 ± 2%, T = 20 ± 2 C°, m_{TiO2} = 26 g.m^{-2})

It should be noted that a summary of the intensification part is highlighted, allowing for a review of this study, the details of which are presented in Figure S1.

3.2. Continuous photoctalytic study

In order to evaluate the performance of the different front flow photocatalytic reactors presented below, many factors have been considered.

The overall rate of photocatalytic degradation is an important factor in evaluating VOC's removal performance. VOC's removal efficiency is defined as:

$$RE\ (\%) = \frac{[\mathrm{VOCs}]in - [\mathrm{VOCs}]out}{[\mathrm{VOCs}]in}\ 100\ \% \qquad \text{(Eq. 3)}$$

The overall rate of photocatalytic degradation of cyclohexane is calculated as:

$$\mathrm{r} = \left(\frac{\mathrm{Q}}{\mathrm{S}}\right)\left(\frac{[\mathrm{VOCs}]in}{100}\right) RE\ (\%) \qquad \text{(Eq. 4)}$$

Where $[VOCs]_{in}$ and $[VOCs]_{out}$ are respectively the inlet and outlet pollutant concentration (mmol/m^3), Q is the volumetric flow rate (L.min^{-1}) and S the mean surface of the catalytic support (m^2).

The overall selectivity of CO_2 can be a useful parameter in evaluating the performance of the photocatalytic reactor with respect to the removal of VOCs. It makes it possible to estimate the rate of mineralization, that is to say the final reaction step of the process. The global selectivity of CO_2 is expressed as follows

$$SCO_2\ (\%) = \frac{[CO_2]out - [CO_2]in}{N_C\ RE\ (\%)\ [\mathrm{VOCs}]in}\ 10^4 \qquad \text{(Eq. 5)}$$

Where $[CO_2]_{in}$ and $[CO_2]_{out}$ refer respectively to the concentration of carbon dioxide at the air inlet and outlet (mmol/m^3). The number N_c represents the stoichiometric coefficient of the overall degradation reaction (in our case, it is equal to 6).

Another criterion considered was the compactness of the reactor. This is an important engineering parameter, as it allows to highlight the efficiency of reactor designs in terms of compactness, which is expressed as the catalytic surface area per unit volume of the reactor (equation 6).

$$Compactness = \frac{Catalytic\ area}{Reactor\ volume} \qquad \text{(Eq. 6)}$$

3.2.1. Comparison of the photocatalytic reactor configurations

This study focuses on the comparison of the cyclohexane removal efficiencies under different inlet concentrations, with the different configurations of front flow photocatalytic reactors (P50, PFR-LED and PFR-LED Optimized). Two key factors were considered; the reactor compactness, as well as the specific degradation rate, expressed in mmol removed per catalyst surface, per unit time, per gram of TiO_2 and per unit of electrical power consumed (Ec) (Figure 8).

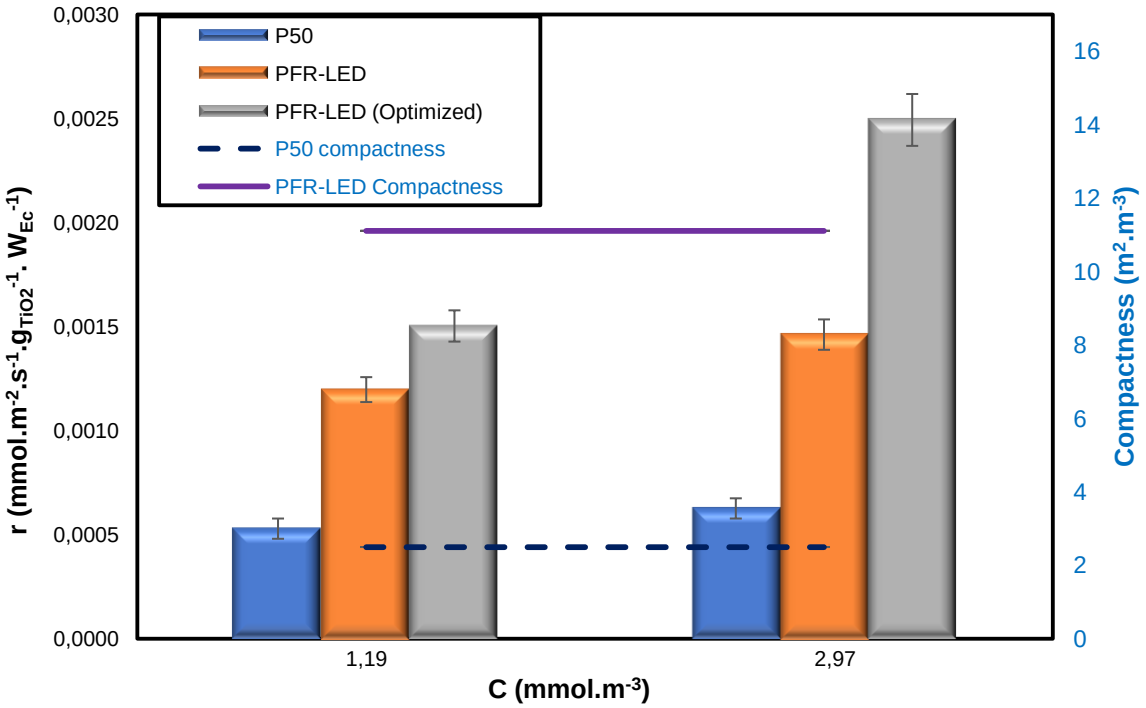

Figure 8: Specific degradation rate and Compactness for the elimination of cyclohexane with P50 (m_{TiO2} 0,64 g, I= 20 W.m^{-2}, Ec = 31.1 W), PFR-LED (m_{TiO2} = 0,3 g, I= 4,5 W.m^{-2}, Ec = 14.5 W), PFR-LED (Optimized) (m_{TiO2} = 0,78 g, I= 7,8 W.m^{-2} Ec = 15.7 W). Q = 18 L.min^{-1}, RH = 38 ± 2 %, T=20 ± 2 °C.

The results show first of all, that the use of lamps inside the reactor as a light source for catalyst activation takes up a lot of space in the reactor. The compacity is 4.5 times higher than for LED reactors [14]. In addition, the system based on the OF

media was clearly more efficient in terms of cyclohexane removal per mass of TiO_2 and watt consumed. The performance of PFR-LEDs could be explained by the lighting efficiency as shown on part 3.1 [28][31][30].

The reactor based on optic fiber media (UV-LED) provides a better treatment capacity than a conventional system (P50), where at a certain UV intensity, the *in-situ* lighting allows a better propagation of the photons, thus allowing the activation of more sites on the surface of the catalyst [21][58]. OF media allows oxidation reactions to occur in a large area of the catalyst, thus increasing the reaction rate [21][59].

The results show that the use of a reactor based on OF media allows the interaction of key features for the photocatalytic reaction to further improve it. In particular the increase of TiO_2 concentration and UV intensity (PFR-LED Optimized) improve the photocatalytic capacity of the reactor for the removal of the pollutant. We note also that at high concentration, and contrary to the simple version of the PFR-LED, the optimized PFR-LED photocatalytic module allowed a better kinetic degradation of the pollutant thanks to its large photocatalytic active surface [47][50].

An energy gain has been proven in this study especially when passing from the conventional configuration to the new configuration based on FO media. Indeed, an improvement about 78% was found, this also highlights the interest of using such a lighting way of photocatalytic sites (*In-situ* lighting). It is also worth mentioning that a comparison in terms of consumed UV watt is developed in order to highlight the energy gain of the process intensification, illustrated in Figure S2.

Thus, the process performance of this last pilot will be studied below.

3.2.2. Performance of the optimized photocatalytic reactor under simulated real conditions

3.2.2.a. Inlet concentration and flow rate effect

In this study, two high concentrations were used (1.19 and 2.97 mmol.m^{-3}) to understand their influence on the performance of the new photocatalytic reactor configuration (PFR-LED Optimized). The removal efficiency of cyclohexane as well as the dependence of the selectivity on different input concentrations under different flow rates are presented in Figure 9.

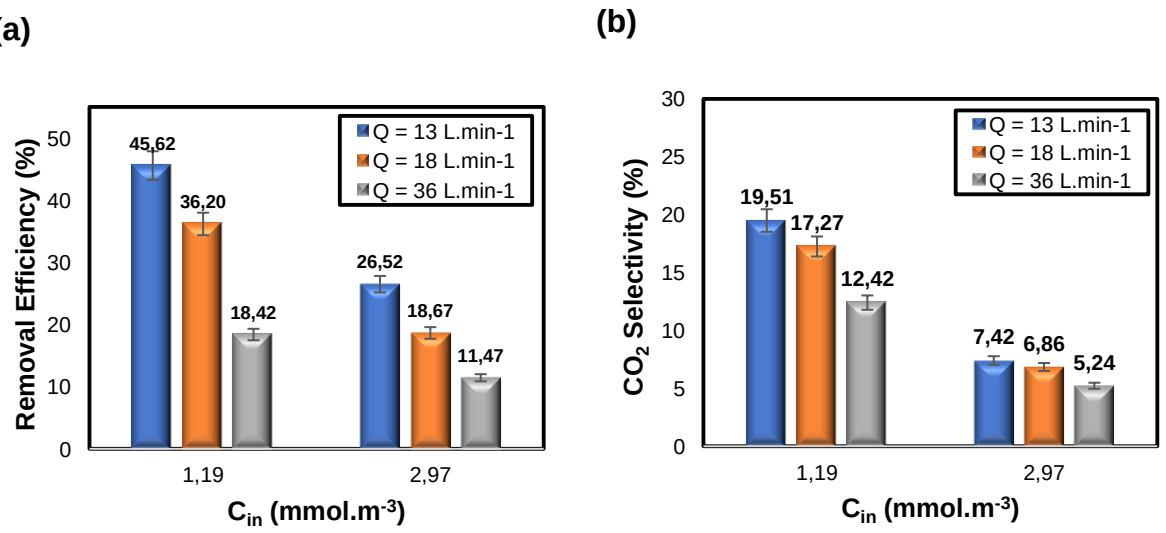

Figure 9: Inlet concentration and flow rate effect on (a) removal efficiency and (b) CO_2 selectivity of the PFR-LED (Optimized): m_{TiO2} = 0,78 g, I= 7,8 w/m^2, HR = 5%, T=20 ± 2 °C.

The results (Fig. 9a) show a similar behavior to what is reported in the literature [60,61], where at a given flow rate, the degradation rate tends to a limit at higher concentration of pollutants. This is related to the limitation by the chemical reaction step due to the unavailability of active sites. It is also recorded that the increase of the flow rate makes the removal efficiency of cyclohexane decrease, due to lowering contact time between the pollutant and the active sites [62][63][64][65].

Figure 9b, shows the dependence of the selectivity on the inlet concentration of Cyclohexane at different flow rates. Either the results agree with what was expected, the influence of the inlet concentration on the CO_2 selectivity is clearly shown. This decrease with increasing pollutant concentration, due to the fact that there are fewer active sites available on the surface of the photocatalyst [54] [63], which also confirms that the process is limited by the availability of active sites. Increasing the flow rate also leads to a decrease in the rate of mineralization. This is due to the fact that the contact time is insufficient for the degradation of the by-products. Adding to this, the competition of the by-products formed towards the active sites reduces the selectivity [66].

Thus, this compact configuration presents excellent performances in terms of pollutant removal with less energy consumption, compared to the classical configuration [33].

3.2.2.b. Relative humidity effect

The effect of humidity on the photocatalytic performance of the new optimized PFR-LED reactor was investigated, under a relative humidity range of 5-80% where an optimum was recorded [67][68][69][70]. The description of this study and the results are detailed in the information support (Fig S3).

3.2.2.b. Effect of the number of compartments

In order to further improve the design of the pilot, the effect of the number of photocatalytic media, i.e. the number of compartments was studied. For this purpose, several combinations using two to four pairs of optical fiber/UV-LED called: 2OF/UV-LED, 3OF/3UV-LED, and 4OF/4UV-LED) were installed. The characteristics of the new optimized configuration are m_{TiO2} = 26 $g.m^{-2}$ and UV intensity = 2.6 $W.m^{-2}$. The

removal profile of Cyclohexane as a function of the number of photocatalytic media (OF/UV-LED), at different input concentrations (1.19 mmol.m^{-3} to 2.97 mmol.m^{-3}) under the optimal relative humidity condition, as well as CO_2 selectivity, are presented in figure 10.

(a)

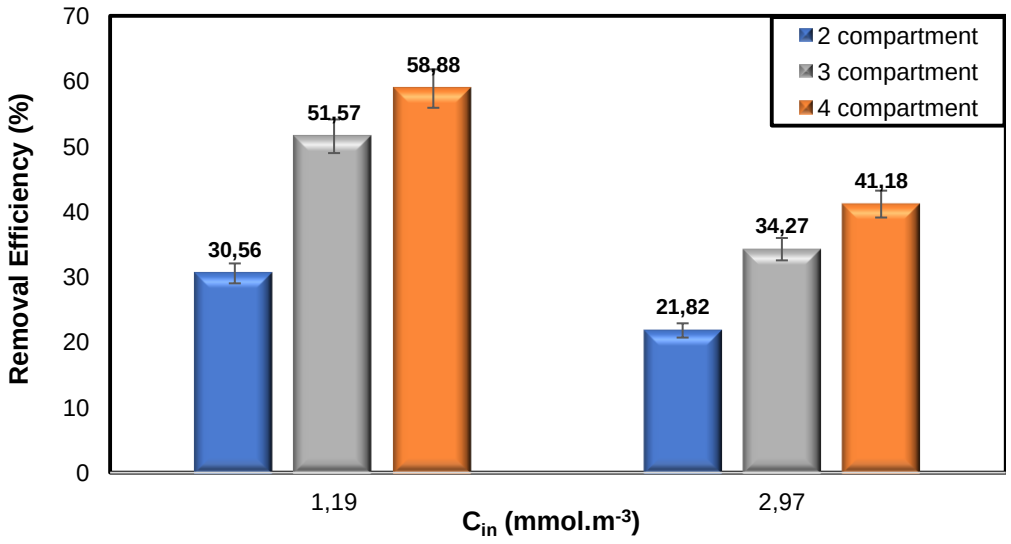

(b)

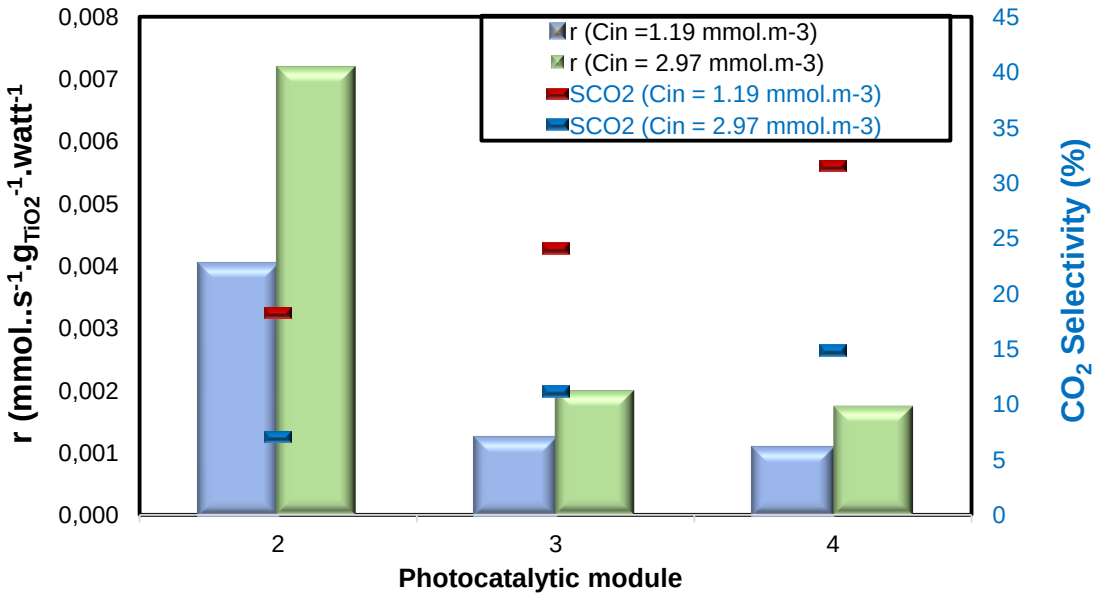

Figure 10: Effect of the number of compartments on (a) removal efficiency and (b)

Specific degradation rate and CO_2 selectivity of the PFR-LED (Optimized): m_{TiO2} $_{media}$= 26 $g.m^{-2}$, I_{media} = 2,6 $W.m^{-2}$, Q = 18 $L.min^{-1}$, RH = 38 ± 2 %, T=20 ± 2 C°

The results in the Fig.10a showed that the oxidation efficiency of cyclohexane increases with the number of photocatalyst media. This behavior is due to the creation of more active sites with the increase of the photocatalyst surface. Also, to the increase of the residence time. The same behavior was previously highlighted by Abidi et al [23] during the treatment of chloroform by a photocatalytic planar reactor based on luminous textile.

The analysis of the specific degradation rate as well as the CO_2 selectivity rate, recorded after each addition of photocatalytic media is added, for the two concentrations studied as shown in Fig. 10b. The results show that the specific degradation rate decreases with the increase of the number of photocatalytic mediums. This is due to the fact that the added OF media receives less pollutant concentration and more by-products, and therefore, the efficiency of the added photocatalyst cannot be at its highest possible performance level [44]. However, the increase of OF media represents a real interest for by-products degradation and leading to better selectivity of the outlet effluent.

4. Conclusions

In this study, an innovative TiO_2 coated OF light fabric was considered for the optimization of the photocatalytic treatment. Results showed that the light textile improves the contact between light, catalyst and pollutant and thus the process efficiency is improved. The intensification of the heterogeneous photocatalysis of TiO_2 under UV-LED irradiation was approved.

This new technology has allowed the development of a new design of frontal flow photocatalytic reactors, with a more compact configuration. The comparison of their performances with those of conventional photocatalytic reactors has shown that the optical fiber technology represents a gain in energy, compactness and photocatalytic efficiency for the removal of cyclohexane compared to conventional systems.

The performance of the optimized version of the front flow photocatalytic reactor (PFR-LED Optimized) was evaluated, where the effect of inlet concentration, flow rate, as well as the complex effect of humidity on the photocatalytic efficiency and mineralization of cyclohexane were shown. In addition, the effect of the number of photocatalytic compartments on the process was highlighted.

Through this study, a new front flow reactor design exhibiting a good energy efficiency and better compactness was developed. The data of this investigation respond perfectly with the requirements of the sustainable development policy, namely affordability and innovation to combat climate change, as stipulated in the sustainable development goals (GSDs) 7 and 9, which respectively target clean and affordable energy as well as industry, innovation and infrastructure.

In addition, this new compact and optimized version could be a real prospect for anti-gas filtration equipment, i.e. gas masks or on-board filtration systems.

5. Acknowledges

The authors gratefully acknowledge the Brochier Technologies (BT) company for its contribution in the supply of luminous textiles samples.

Reference:

[1] C. Stewart, D.E. Damby, C.J. Horwell, T. Elias, E. Ilyinskaya, I. Tomašek, B.M.

Longo, A. Schmidt, H.K. Carlsen, E. Mason, P.J. Baxter, S. Cronin, C. Witham, Volcanic air pollution and human health: recent advances and future directions, Bull. Volcanol. 84 (2022). https://doi.org/10.1007/s00445-021-01513-9.

[2] S.S. Purohit, A.K. Agrawal, Environmental Pollution: Causes, Effects and Control, (2021).

[3] A. Luengas, A. Barona, C. Hort, G. Gallastegui, V. Platel, A. Elias, A review of indoor air treatment technologies, Rev. Environ. Sci. Biotechnol. 14 (2015) 499–522. https://doi.org/10.1007/s11157-015-9363-9.

[4] J. González-Martín, N.J.R. Kraakman, C. Pérez, R. Lebrero, R. Muñoz, A state–of–the-art review on indoor air pollution and strategies for indoor air pollution control, Chemosphere. 262 (2021). https://doi.org/10.1016/j.chemosphere.2020.128376.

[5] V.K.H. Bui, T.N. Nguyen, V. Van Tran, J. Hur, I.T. Kim, D. Park, Y.C. Lee, Photocatalytic materials for indoor air purification systems: An updated mini-review, Environ. Technol. Innov. 22 (2021) 101471. https://doi.org/10.1016/j.eti.2021.101471.

[6] F. He, W. Jeon, W. Choi, Photocatalytic air purification mimicking the self-cleaning process of the atmosphere, Nat. Commun. 12 (2021) 10–13. https://doi.org/10.1038/s41467-021-22839-0.

[7] B. Bakbolat, C. Daulbayev, F. Sultanov, R. Beissenov, A. Umirzakov, A. Mereke, A. Bekbaev, I. Chuprakov, Recent developments of TiO2-based photocatalysis in the hydrogen evolution and photodegradation: A review, Nanomaterials. 10 (2020) 1–16. https://doi.org/10.3390/nano10091790.

[8] A. Talaiekhozani, S. Rezania, K.H. Kim, R. Sanaye, A.M. Amani, Recent

advances in photocatalytic removal of organic and inorganic pollutants in air, J. Clean. Prod. 278 (2021) 123895. https://doi.org/10.1016/j.jclepro.2020.123895.

[9] M. Malayeri, F. Haghighat, C.S. Lee, Modeling of volatile organic compounds degradation by photocatalytic oxidation reactor in indoor air: A review, Build. Environ. 154 (2019) 309–323. https://doi.org/10.1016/j.buildenv.2019.02.023.

[10] Y. Boyjoo, H. Sun, J. Liu, V.K. Pareek, S. Wang, A review on photocatalysis for air treatment: From catalyst development to reactor design, Chem. Eng. J. 310 (2017) 537–559. https://doi.org/10.1016/j.cej.2016.06.090.

[11] C. McCullagh, N. Skillen, M. Adams, P.K.J. Robertson, Photocatalytic reactors for environmental remediation: A review, J. Chem. Technol. Biotechnol. 86 (2011) 1002–1017. https://doi.org/10.1002/jctb.2650.

[12] G. Maxime, A. Aymen Amine, B. Abdelkrim, W. Dominique, Removal of gas-phase ammonia and hydrogen sulfide using photocatalysis, nonthermal plasma, and combined plasma and photocatalysis at pilot scale, Environ. Sci. Pollut. Res. 21 (2014) 13127–13137. https://doi.org/10.1007/s11356-014-3244-6.

[13] A.A. Assadi, A. Bouzaza, D. Wolbert, Comparative study between laboratory and large pilot scales for VOC’s removal from gas streams in continuous flow surface discharge plasma, Chem. Eng. Res. Des. 106 (2016) 308–314. https://doi.org/10.1016/j.cherd.2015.12.025.

[14] G.C. Roda, V. Loddo, L. Palmisano, F. Parrino, Special needs and characteristic features of (photo)catalytic reactors with a review of the proposed Solutions, Elsevier B.V., 2019. https://doi.org/10.1016/B978-0-444-64015-4.00006-7.

[15] F. Khodadadian, A. Poursaeidesfahani, Z. Li, J.R. van Ommen, A.I. Stankiewicz, R. Lakerveld, Model-Based Optimization of a Photocatalytic Reactor with Light-Emitting Diodes, Chem. Eng. Technol. 39 (2016) 1946–1954. https://doi.org/10.1002/ceat.201600010.

[16] W.K. Jo, R.J. Tayade, New generation energy-efficient light source for photocatalysis: LEDs for environmental applications, Ind. Eng. Chem. Res. 53 (2014) 2073–2084. https://doi.org/10.1021/ie404176g.

[17] Y.T. Wu, Y.H. Yu, V.H. Nguyen, K. Te Lu, J.C.S. Wu, L.M. Chang, C.W. Kuo, Enhanced xylene removal by photocatalytic oxidation using fiber-illuminated honeycomb reactor at ppb level, J. Hazard. Mater. 262 (2013) 717–725. https://doi.org/10.1016/j.jhazmat.2013.09.037.

[18] K. Te Lu, V.H. Nguyen, Y.H. Yu, C.C. Yu, J.C.S. Wu, L.M. Chang, A.Y.C. Lin, An internal-illuminated monolith photoreactor towards efficient photocatalytic degradation of ppb-level isopropyl alcohol, Chem. Eng. J. 296 (2016) 11–18. https://doi.org/10.1016/j.cej.2016.03.097.

[19] W. Choi, J.Y. Ko, H. Park, J.S. Chung, Investigation on tio2-coated optical fibers for gas-phase photocatalytic oxidation of acetone, Appl. Catal. B Environ. 31 (2001) 209–220. https://doi.org/10.1016/S0926-3373(00)00281-2.

[20] R. De Sun, A. Nakajima, I. Watanabe, T. Watanabe, K. Hashimoto, TiO2-coated optical fiber bundles used as a photocatalytic filter for decomposition of gaseous organic compounds, J. Photochem. Photobiol. A Chem. 136 (2000) 111–116. https://doi.org/10.1016/S1010-6030(00)00330-0.

[21] M. Dell'Edera, C. Lo Porto, I. De Pasquale, F. Petronella, M.L. Curri, A. Agostiano, R. Comparelli, Photocatalytic TiO2-based coatings for

environmental applications, Catal. Today. 380 (2021) 62–83. https://doi.org/10.1016/j.cattod.2021.04.023.

[22] T. Claes, A. Dilissen, M.E. Leblebici, T. Van Gerven, Translucent packed bed structures for high throughput photocatalytic reactors, Chem. Eng. J. 361 (2019) 725–735. https://doi.org/10.1016/j.cej.2018.12.107.

[23] M. Abidi, A. Hajjaji, A. Bouzaza, L. Lamaa, L. Peruchon, C. Brochier, S. Rtimi, D. Wolbert, B. Bessais, A. Amin Assadi, Modeling of indoor air treatment using an innovative photocatalytic luminous textile: reactor compactness and mass transfer enhancement, Chem. Eng. J. (2021) 132636. https://doi.org/10.1016/j.cej.2021.132636.

[24] O. Debono, V. Gaudion, N. Redon, N. Locoge, F. Thevenet, Photocatalytic treatment of VOC industrial emissions: IPA removal using a sensor-instrumented reactor, Chem. Eng. J. 353 (2018) 394–409. https://doi.org/10.1016/j.cej.2018.07.151.

[25] M. Malayeri, F. Haghighat, C.S. Lee, Kinetic modeling of the photocatalytic degradation of methyl ethyl ketone in air for a continuous-flow reactor, Chem. Eng. J. 404 (2021) 126602. https://doi.org/10.1016/j.cej.2020.126602.

[26] J. Oliveira De Brito Lira, H.G. Riella, N. Padoin, C. Soares, An Overview of Photoreactors and Computational Modeling for the Intensification of Photocatalytic Processes in the Gas-Phase: State-of-Art, J. Environ. Chem. Eng. 9 (2021). https://doi.org/10.1016/j.jece.2021.105068.

[27] W. Abou Saoud, A. Kane, P. Le Cann, A. Gerard, L. Lamaa, L. Peruchon, C. Brochier, A. Bouzaza, D. Wolbert, A.A. Assadi, Innovative photocatalytic reactor for the degradation of VOCs and microorganism under simulated indoor

575 air conditions: Cu-Ag/TiO2-based optical fibers at a pilot scale, Chem. Eng. J.
576 411 (2021) 128622. https://doi.org/10.1016/j.cej.2021.128622.

577 [28] C. Indermühle, E. Puzenat, F. Simonet, L. Peruchon, C. Brochier, C. Guillard,
578 Modelling of UV optical ageing of optical fibre fabric coated with TiO2, Appl.
579 Catal. B Environ. 182 (2016) 229–235.
580 https://doi.org/10.1016/j.apcatb.2015.09.037.

581 [29] P.A. Bourgeois, E. Puzenat, L. Peruchon, F. Simonet, D. Chevalier, E. Deflin,
582 C. Brochier, C. Guillard, Characterization of a new photocatalytic textile for
583 formaldehyde removal from indoor air, Appl. Catal. B Environ. 128 (2012) 171–
584 178. https://doi.org/10.1016/j.apcatb.2012.03.033.

585 [30] A. Almansba, A. Kane, N. Nasrallah, R. Maachi, L. Lamaa, L. Peruchon, C.
586 Brochier, I. Béchohra, A. Amrane, A.A. Assadi, Innovative photocatalytic
587 luminous textiles optimized towards water treatment: Performance evaluation
588 of photoreactors, Chem. Eng. J. 416 (2021).
589 https://doi.org/10.1016/j.cej.2021.129195.

590 [31] A. Almansba, A. Kane, N. Nasrallah, J.M. Wilson, R. Maachi, L. Lamaa, L.
591 Peruchon, C. Brochier, A. Amrane, A.A. Assadi, An engineering approach
592 towards the design of an innovative compact photo-reactor for antibiotic
593 removal in the frame of laboratory and pilot-plant scale, J. Photochem.
594 Photobiol. A Chem. 418 (2021) 113445.
595 https://doi.org/10.1016/j.jphotochem.2021.113445.

596 [32] S. Karoui, R. Ben Arfi, A. Ghorbal, A. Amrane, A.A. Assadi, Innovative
597 sequential combination of fixed bed adsorption/desorption and photocatalysis
598 cost-effective process to remove antibiotics in solution, Prog. Org. Coatings.

151 (2021) 106014. https://doi.org/10.1016/j.porgcoat.2020.106014.

[33] Y. Serhane, N. Belkessa, A. Bouzaza, D. Wolbert, A.A. Assadi, Continuous air purification by front flow photocatalytic reactor: Modelling of the influence of mass transfer step under simulated real conditions, Chemosphere. 295 (2022) 133809. https://doi.org/10.1016/j.chemosphere.2022.133809.

[34] A.A. Assadi, J. Palau, A. Bouzaza, D. Wolbert, Modeling of a continuous photocatalytic reactor for isovaleraldehyde oxidation: Effect of different operating parameters and chemical degradation pathway, Chem. Eng. Res. Des. 91 (2013) 1307–1316. https://doi.org/10.1016/j.cherd.2013.02.020.

[35] P. Mazierski, J. Nadolna, W. Lisowski, M.J. Winiarski, M. Gazda, M. Nischk, T. Klimczuk, A. Zaleska-Medynska, Effect of irradiation intensity and initial pollutant concentration on gas phase photocatalytic activity of TiO2 nanotube arrays, Catal. Today. 284 (2017) 19–26. https://doi.org/10.1016/j.cattod.2016.09.004.

[36] M. Abidi, A. Hajjaji, A. Bouzaza, K. Trablesi, H. Makhlouf, S. Rtimi, A.A. Assadi, B. Bessais, Simultaneous removal of bacteria and volatile organic compounds on Cu2O-NPs decorated TiO2 nanotubes: Competition effect and kinetic studies, J. Photochem. Photobiol. A Chem. 400 (2020). https://doi.org/10.1016/j.jphotochem.2020.112722.

[37] W. Elfalleh, A.A. Assadi, A. Bouzaza, D. Wolbert, J. Kiwi, S. Rtimi, Innovative and stable TiO2 supported catalytic surfaces removing aldehydes under UV-light irradiation, J. Photochem. Photobiol. A Chem. 343 (2017) 96–102. https://doi.org/10.1016/j.jphotochem.2017.04.029.

[38] O. Debono, V. Hequet, L. Le Coq, N. Locoge, F. Thevenet, VOC ternary

623 mixture effect on ppb level photocatalytic oxidation: Removal kinetic, reaction
624 intermediates and mineralization, Appl. Catal. B Environ. 218 (2017) 359–369.
625 https://doi.org/10.1016/j.apcatb.2017.06.070.

626 [39] R.E. Stroe, L.A. Rosendahl, Kinetic study of the photocatalytic oxidation of
627 ethylene over TiO2 thin films, IOP Conf. Ser. Mater. Sci. Eng. 628 (2019).
628 https://doi.org/10.1088/1757-899X/628/1/012009.

629 [40] D.S. Selishchev, T.N. Filippov, M.N. Lyulyukin, D. V. Kozlov, Uranyl-modified
630 TiO2 for complete photocatalytic oxidation of volatile organic compounds under
631 UV and visible light, Chem. Eng. J. 370 (2019) 1440–1449.
632 https://doi.org/10.1016/j.cej.2019.03.280.

633 [41] B.A. Marinho, R. Djellabi, R.O. Cristóvão, J.M. Loureiro, R.A.R. Boaventura,
634 M.M. Dias, J.C.B. Lopes, V.J.P. Vilar, Intensification of heterogeneous TiO2
635 photocatalysis using an innovative micro–meso-structured-reactor for Cr(VI)
636 reduction under simulated solar light, Chem. Eng. J. 318 (2017) 76–88.
637 https://doi.org/10.1016/j.cej.2016.05.077.

638 [42] Y. Li, S. Wang, Q. Chen, Potential of thirteen urban greening plants to capture
639 particulate matter on leaf surfaces across three levels of ambient atmospheric
640 pollution, Int. J. Environ. Res. Public Health. 16 (2019).
641 https://doi.org/10.3390/ijerph16030402.

642 [43] E. Ahmadi, B. Shokri, A. Mesdaghinia, R. Nabizadeh, M. Reza Khani, S.
643 Yousefzadeh, M. Salehi, K. Yaghmaeian, Synergistic effects of α-Fe2O3-TiO2
644 and Na2S2O8 on the performance of a non-thermal plasma reactor as a novel
645 catalytic oxidation process for dimethyl phthalate degradation, Sep. Purif.
646 Technol. 250 (2020) 117185. https://doi.org/10.1016/j.seppur.2020.117185.

[44] M. Malayeri, F. Haghighat, C.S. Lee, Modeling of volatile organic compounds degradation by photocatalytic oxidation reactor in indoor air: A review, Build. Environ. 154 (2019) 309–323. https://doi.org/10.1016/j.buildenv.2019.02.023.

[45] Y.W. Li, W.L. Ma, Photocatalytic oxidation technology for indoor air pollutants elimination: A review, Chemosphere. 280 (2021) 130667. https://doi.org/10.1016/j.chemosphere.2021.130667.

[46] A. Alonso-Tellez, R. Masson, D. Robert, N. Keller, V. Keller, Comparison of Hombikat UV100 and P25 TiO 2 performance in gas-phase photocatalytic oxidation reactions, J. Photochem. Photobiol. A Chem. 250 (2012) 58–65. https://doi.org/10.1016/j.jphotochem.2012.10.008.

[47] X. Wang, L. Jiang, K. Li, J. Wang, D. Fang, Y. Zhang, D. Tian, Z. Zhang, D.D. Dionysiou, Fabrication of novel Z-scheme SrTiO3/MnFe2O4 system with double-response activity for simultaneous microwave-induced and photocatalytic degradation of tetracycline and mechanism insight, Chem. Eng. J. 400 (2020) 125981. https://doi.org/10.1016/j.cej.2020.125981.

[48] M. Vezzoli, T. Farrell, A. Baker, S. Psaltis, W.N. Martens, J.M. Bell, Optimal catalyst thickness in titanium dioxide fixed film reactors: Mathematical modelling and experimental validation, Chem. Eng. J. 234 (2013) 57–65. https://doi.org/10.1016/j.cej.2013.08.049.

[49] X. Yue, N.L. Ma, C. Sonne, R. Guan, S.S. Lam, Q. Van Le, X. Chen, Y. Yang, H. Gu, J. Rinklebe, W. Peng, Mitigation of indoor air pollution: A review of recent advances in adsorption materials and catalytic oxidation, J. Hazard. Mater. 405 (2021). https://doi.org/10.1016/j.jhazmat.2020.124138.

[50] M. Jafarikojour, M. Sohrabi, S.J. Royaee, A. Hassanvand, Evaluation and

671 Optimization of a Novel Immobilized Photoreactor for the Degradation of
672 Gaseous Toluene, Clean - Soil, Air, Water. 43 (2015) 662–670.
673 https://doi.org/10.1002/clen.201300985.

674 [51] M.E. Leblebici, J. Rongé, J.A. Martens, G.D. Stefanidis, T. Van Gerven,
675 Computational modelling of a photocatalytic UV-LED reactor with internal mass
676 and photon transfer consideration, Chem. Eng. J. 264 (2015) 962–970.
677 https://doi.org/10.1016/j.cej.2014.12.013.

678 [52] Z. Shayegan, C.S. Lee, F. Haghighat, TiO2 photocatalyst for removal of volatile
679 organic compounds in gas phase – A review, Chem. Eng. J. 334 (2018) 2408–
680 2439. https://doi.org/10.1016/j.cej.2017.09.153.

681 [53] A.H. Mamaghani, F. Haghighat, C.S. Lee, Photocatalytic oxidation technology
682 for indoor environment air purification: The state-of-the-art, Appl. Catal. B
683 Environ. 203 (2017) 247–269. https://doi.org/10.1016/j.apcatb.2016.10.037.

684 [54] A.A. Assadi, A. Bouzaza, D. Wolbert, P. Petit, Isovaleraldehyde elimination by
685 UV/TiO<inf>2</inf> photocatalysis: comparative study of the process at
686 different reactors configurations and scales, Environ. Sci. Pollut. Res. 21
687 (2014) 11178–11188. https://doi.org/10.1007/s11356-014-2603-7.

688 [55] L. Zhong, F. Haghighat, C.S. Lee, Ultraviolet photocatalytic oxidation for indoor
689 environment applications: Experimental validation of the model, Build. Environ.
690 62 (2013) 155–166. https://doi.org/10.1016/j.buildenv.2013.01.009.

691 [56] X. Wang, X. Tan, T. Yu, Modeling of formaldehyde photocatalytic degradation
692 in a honeycomb monolith reactor using computational fluid dynamics, Ind. Eng.
693 Chem. Res. 53 (2014) 18402–18410. https://doi.org/10.1021/ie5016427.

694 [57] Z. Wang, J. Liu, Y. Dai, W. Dong, S. Zhang, J. Chen, CFD modeling of a UV-

LED photocatalytic odor abatement process in a continuous reactor, J. Hazard. Mater. 215–216 (2012) 25–31. https://doi.org/10.1016/j.jhazmat.2012.02.021.

[58] Y. Song, L. Ling, P. Westerhoff, C. Shang, Evanescent waves modulate energy efficiency of photocatalysis within TiO2 coated optical fibers illuminated using LEDs, Nat. Commun. 12 (2021) 1–9. https://doi.org/10.1038/s41467-021-24370-8.

[59] A.H. Mamaghani, F. Haghighat, C.S. Lee, Effect of titanium dioxide properties and support material on photocatalytic oxidation of indoor air pollutants, Build. Environ. 189 (2021) 107518. https://doi.org/10.1016/j.buildenv.2020.107518.

[60] W. Abou Saoud, A.A. Assadi, M. Guiza, A. Bouzaza, W. Aboussaoud, I. Soutrel, A. Ouederni, D. Wolbert, S. Rtimi, Abatement of ammonia and butyraldehyde under non-thermal plasma and photocatalysis: Oxidation processes for the removal of mixture pollutants at pilot scale, Chem. Eng. J. 344 (2018) 165–172. https://doi.org/10.1016/j.cej.2018.03.068.

[61] W. Abou Saoud, A.A. Assadi, M. Guiza, A. Bouzaza, W. Aboussaoud, A. Ouederni, I. Soutrel, D. Wolbert, S. Rtimi, Study of synergetic effect, catalytic poisoning and regeneration using dielectric barrier discharge and photocatalysis in a continuous reactor: Abatement of pollutants in air mixture system, Appl. Catal. B Environ. 213 (2017) 53–61. https://doi.org/10.1016/j.apcatb.2017.05.012.

[62] A.H. Mamaghani, F. Haghighat, C.S. Lee, Photocatalytic degradation of VOCs on various commercial titanium dioxides: Impact of operating parameters on removal efficiency and by-products generation, Build. Environ. 138 (2018) 275–282. https://doi.org/10.1016/j.buildenv.2018.05.002.

[63] T. Zadi, M. Azizi, N. Nasrallah, A. Bouzaza, R. Maachi, D. Wolbert, S. Rtimi, A.A. Assadi, Indoor air treatment of refrigerated food chambers with synergetic association between cold plasma and photocatalysis: Process performance and photocatalytic poisoning, Chem. Eng. J. 382 (2020) 122951. https://doi.org/10.1016/j.cej.2019.122951.

[64] A.A. Assadi, A. Bouzaza, D. Wolbert, Study of synergetic effect by surface discharge plasma/TiO2 combination for indoor air treatment: Sequential and continuous configurations at pilot scale, J. Photochem. Photobiol. A Chem. 310 (2015) 148–154. https://doi.org/10.1016/j.jphotochem.2015.05.007.

[65] J. Palau, A.A. Assadi, J.M. Penya-Roja, A. Bouzaza, D. Wolbert, V. Martínez-Soria, Isovaleraldehyde degradation using UV photocatalytic and dielectric barrier discharge reactors, and their combinations, J. Photochem. Photobiol. A Chem. 299 (2015) 110–117. https://doi.org/10.1016/j.jphotochem.2014.11.013.

[66] A.A. Assadi, A. Bouzaza, D. Wolbert, Photocatalytic oxidation of trimethylamine and isovaleraldehyde in an annular reactor: Influence of the mass transfer and the relative humidity, J. Photochem. Photobiol. A Chem. 236 (2012) 61–69. https://doi.org/10.1016/j.jphotochem.2012.03.020.

[67] G. Zhang, Y. Liu, Z. Hashisho, Z. Sun, S. Zheng, L. Zhong, Adsorption and photocatalytic degradation performances of TiO2/diatomite composite for volatile organic compounds: Effects of key parameters, Appl. Surf. Sci. 525 (2020). https://doi.org/10.1016/j.apsusc.2020.146633.

[68] J. Chen, G. Li, Z. He, T. An, Adsorption and degradation of model volatile organic compounds by a combined titania-montmorillonite-silica photocatalyst, J. Hazard. Mater. 190 (2011) 416–423.

https://doi.org/10.1016/j.jhazmat.2011.03.064.

[69] A.M. Vandenbroucke, R. Morent, N. De Geyter, C. Leys, Non-thermal plasmas for non-catalytic and catalytic VOC abatement, J. Hazard. Mater. 195 (2011) 30–54. https://doi.org/10.1016/j.jhazmat.2011.08.060.

[70] T. Martinez, A. Bertron, G. Escadeillas, E. Ringot, V. Simon, BTEX abatement by photocatalytic TiO2-bearing coatings applied tocement mortars, Build. Environ. 71 (2014) 186–192. https://doi.org/10.1016/j.buildenv.2013.10.004.